International Journal of Heat and Mass Transfer 52 (2009) 5046–5054

Contents lists available at ScienceDirect

International Journal of Heat and Mass Transfer

journal homepage: www.elsevier.com/locate/ijhmt

Fluid-to-fluid modeling of supercritical water loops for stability analysis

C.P. Marcel *, M. Rohde, V.P. Masson [1], T.H.J.J. Van der Hagen

Department of Physics of Nuclear Reactors, Delft University of Technology, Mekelweg 15, Delft 2629 JB, The Netherlands

ARTICLE INFO

Article history:
Received 22 October 2007
Accepted 24 March 2009
Available online 21 June 2009

Keywords:
Fluid-to-fluid modeling
Stability
Supercritical water nuclear reactor

ABSTRACT

The use of supercritical water as coolant/moderator may induce oscillations in the supercritical light water reactor similar to the density wave oscillations observed in boiling water reactors (BWRs). In order to experimentally investigate the stability of supercritical reactors, a fluid-to-fluid downscaled facility is proposed. It is found that with an appropriate mixture of refrigerants R-125 and R-32, the dimensionless enthalpy and density of the supercritical water can be accurately matched for all relevant operational conditions of the reactor. Moreover, the inertia distribution, the friction factor distribution and the heat transfer mechanism are taken into account in the modeling. As a result of the proposed downscaling, the operational pressure, temperature and power are considerably smaller than those of a water-based system, which in turn helps reducing the construction and operational costs of a test facility. Finally, it is found that the often used modeling fluid supercritical CO_2 cannot accurately represent supercritical water at reactor conditions.

1. Introduction

The supercritical light water reactor belongs to the group of the most promising reactor designs selected in the Generation-IV international advanced nuclear reactor development program [1]. This reactor design is characterized by its inherently high thermodynamic efficiency (~45%) and the fact it uses water in supercritical state as a coolant.

In nuclear reactors, great attention has to be paid to the characterization of the stability performance since instabilities may strongly degrade the safety of the plant. In the case of the supercritical water reactor, little is known regarding the physical mechanisms that may affect the stability. For instance, the density change in supercritical water systems exceeds that in typical BWR cores: in a typical supercritical water reactor core, the coolant density changes from 780 to 90 kg m^{-3} while in typical Boling Water Reactors (BWRs) the coolant density changes from 750 to 198 kg m^{-3}. Therefore, density wave oscillations [2] can play an important role in determining the thermal-hydraulic stability of such systems. Thorough fundamental investigations are needed on the stability performance of nuclear reactors working with supercritical water as a coolant.

In this work, the European High Performance Light Water Nuclear Reactor (HPLWR) [3] is taken as the reference supercritical water reactor design. The first attempts to numerically investigate the thermal-hydraulic stability of the HPLWR have shown contradictory results which are not yet fully understood. In particular, the *near-peak* stability margin region (in the steady state flow–power curve), see Chatoorgoon [4], has not been observed by other authors and it is proposed to be caused by dissipative and dispersive effects in the numerical model (see Jain [5] and Ortega Gómez et al. [6]). Benchmarking the numerical results for conditions relevant to the HPLWR is difficult since accurate experimental data are lacking. New experimental campaigns need to be performed. Such experiments, however, are difficult to assess because of the severe conditions involving supercritical water, leading to considerable construction and operational costs of a water-based test facility. For this reason, a fluid-to-fluid modeling approach is proposed in this work. Fluid-to-fluid downscaling has been applied in the past for simulating boiling processes such as those occurring in BWRs (see, for instance, Lahey and Moody [7] or Van de Graaf and Van der Hagen [8]). For stability investigations of boiling systems, Marcel et al. [9] have derived rules that need to be fulfilled in order to have a proper similarity between the original water system and its downscaled version. To the authors' knowledge, in the case of supercritical systems, a fluid-to-fluid downscaling approach has never been applied, nor have scaling rules been derived.

In this work the scaling rules that need to be used to model the stability of systems operating with supercritical water are derived. Additionally a mixture of fluids capable to simulate supercritical water is proposed. The main differences between the downscaling of supercritical water loops and the downscaling of boiling loops are discussed in the last section of the paper.

* Corresponding author. Tel.: +31 15 278 3811; fax: +31 15 278 6422.
E-mail address: c.p.marcel@tudelft.nl (C.P. Marcel).
[1] CONICET, CNEA, Av. Bustillo 9500, S. C. Bariloche, Argentina.

0017-9310/$ - see front matter © 2009 Published by Elsevier Ltd.
doi:10.1016/j.ijheatmasstransfer.2009.03.022

Nomenclature

Normal alphabet

A	cross-sectional area (m^2)
C_p	heat capacity at constant pressure (kJ kg^{-1} K^{-1})
D	diameter (m)
K	local pressure drop coefficient (–)
L	length (m)
f	frictional factor (–)
g	gravitational acceleration (m s^{-2})
G	mass flux density (kg m^{-2} s^{-1})
h	enthalpy (kJ kg^{-1})
$\hbar$	heat transfer coefficient (kW m^{-2} K^{-1})
k	thermal conductivity (kW m^{-1} K^{-1})
p	pressure (kg m^{-1} s^{-2})
q'	linear power transferred from fuel to coolant (J s^{-1} m^{-1})
q''	surface heat flux (J s^{-1} m^{-2})
r	radius (m)
t	time (s)
T	temperature (°C)
X	scaling factor
Z	axial position (m)

Greek letters

ρ	density (kg m^{-3})
μ	viscosity (Pa s)
v	dynamic viscosity (m^2 s^{-1})

Non-dimensional numbers

N_{PCH}	pseudo phase change number $N_{PCH} \equiv \frac{q'_{tot} L_C}{G_0 h_0 A_c}$
N_{Fr}	Froude number $N_{Fr} \equiv \frac{G_0^2}{\rho_0^2 g D_h}$
N_{Nu}	Nusselt number $N_{Nu} \equiv \frac{\hbar D}{k}$
N_{Pr}	Prandtl number $N_{\mathrm{Pr}} \equiv \frac{\mu C_P}{k}$
N_{Nu}	Reynolds number $N_{\mathrm{Re}} \equiv \frac{G_0 D}{\mu}$

Subscripts and superscripts

*	dimensionless
0	characteristic value
A	area
C	core
g	geometry
h	hydraulic (diameter)
G	mass flux
m	bulk
Pow	power
Press	pressure
rod	regarding one fuel pin rod
s	surface
t	time
tot	relative to the whole facility

2. Fluid-to-fluid scaling procedure for supercritical water loops

Fluid-to-fluid scaling is based on the fact that two systems, represented by analogous differential equations and boundary conditions, have to show the same physical behavior. Based on this idea, the mass, momentum and energy conservation differential equations are mathematically manipulated in order to find the intrinsic parameters that define the problem. By selecting a fluid different than water, while keeping all those parameters the same, may help to reduce, for instance, the power and the pressure required to run a loop representing the reactor.

Fig. 1 shows a schematic view of the scaling procedure proposed in this work. This figure has to be read from top to bottom and from left to right.

The whole scaling process starts with the linear momentum, energy and mass balance equations. The dimensionless form of the differential balance equation for the linear momentum of a fluid flowing through a channel can be expressed by

$$\frac{\partial}{\partial t^*}(G^* A^*) + \frac{\partial}{\partial z^*}\left(\frac{G^{*2} A^*}{\rho^*_{(z)}}\right) + \frac{f_{(z)}}{D^*_h}\frac{G^{*2} A^*}{\rho^*_{(z)}} + \frac{1}{N_{Fr}}\rho^*_{(z)} A^* . \cos\theta + \frac{K_i}{2} A^* \times \frac{G^{*2}}{\rho^*_{(z)}}\delta(z^* - z^*_i) = A^* \frac{\partial}{\partial z^*}(p^*) \quad (1)$$

where θ is the angle of the section with respect to the vertical direction and the dimensionless quantities, denoted by the superindex '*', are defined as

$$t^* = \frac{t}{\frac{L_C \rho_0}{G_0}}, \quad \rho^* = \frac{\rho}{\rho_0}, \quad h^* = \frac{h}{h_0}, \quad G^* = \frac{G}{G_0}, \quad N_{Fr} = \left(\frac{G_0}{\rho_0}\right)^2 \frac{1}{L_C g}, \quad p^* = \frac{p}{\frac{G_0^2}{\rho_0}}, \quad A^* = \frac{A}{L_C^2}, \quad z^* = \frac{z}{L_C} \quad \text{and} \quad D^*_h = \frac{D_h}{L_C} \quad (2)$$

where t stands for the time, L_c for the core length, G for the mass flux density, ρ for the fluid density, h for the enthalpy, N_{Fr} for the Froude number, g for the gravitational acceleration, p for the pressure, A for the cross-sectional area, z for the axial variable, D_h for the hydraulic diameter, f for the friction coefficient and K_i for the friction coefficients of the local restrictions placed at $z = z_i$. The subindex '0' refers to the reference quantities, which in this work correspond to the core inlet.

Similarly, the dimensionless differential mass and energy balance equations are given by

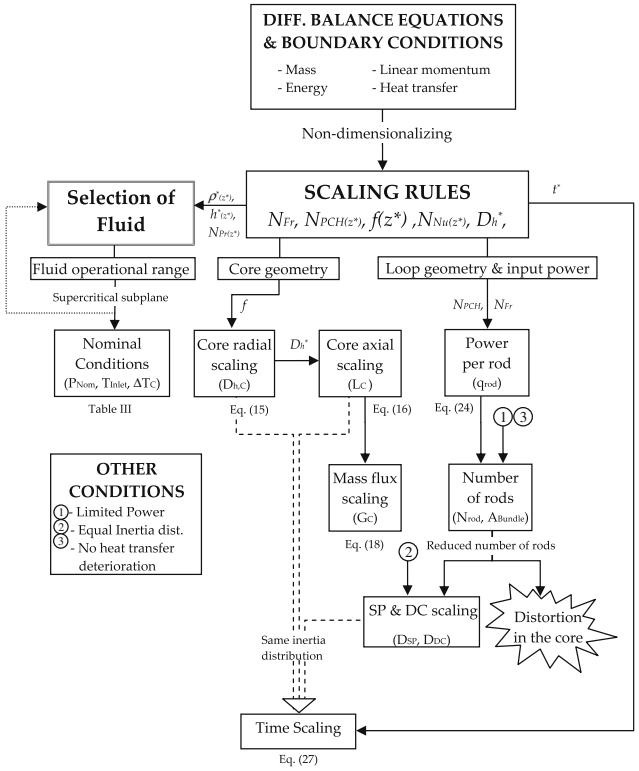

Fig. 1. Block diagram of the scaling procedure.

$$\frac{\partial}{\partial t^*}(\rho^*_{(z)}A^*) + \frac{\partial}{\partial z^*}(G^*A^*) = 0 \tag{3}$$

$$\frac{\partial}{\partial t^*}(\rho^*_{(z)}h^*_{(z)}A^*) + \frac{\partial}{\partial z^*}(G^*h^*_{(z)}A^*) = N_{PCH} \tag{4}$$

where the (pseudo) phase change number is defined as

$$N_{PCH} = \frac{q'L_C}{G_0 h_0 A} \tag{5}$$

q' being the linear power.

Note that the axial dependency of the fluid properties has to be maintained in the equations.

The heat transfer mechanism taking place when the supercritical water fluid cools the reactor fuel rods may affect the stability of the system. For that reason, the heat transfer mechanism in the facility has to be analogous to that occurring in the reactor core. In this way a similar core radial (dimensionless) temperature profile in the reactor and in the downscaled system will be obtained. By using the dimensionless form of the Fourier's law and the definition of the heat transfer coefficient, the following relation can be written (see Appendix for the derivation).

$$\left.\frac{\partial T^*_{(z*)}}{\partial r^*}\right|_{r=r_0} \frac{1}{(T^*_{s(z^*)} - T^*_{m(z^*)})} = \frac{N_{Nu_{(z^*)}}}{2} \tag{6}$$

where r is the radial coordinate, T the temperature and N_{Nu} is the Nusselt number defined as

$$N_{Nu} \equiv \frac{\hbar D}{k} \tag{7}$$

$\hbar$ being the heat transfer coefficient and k the fluid thermal conductivity.

Eq. (6) shows that, in order to have the same radial temperature profile, the two systems have to have the same N_{Nu} at any location in terms of the dimensionless axial position.

N_{Nu} can be interpreted as the dimensionless temperature gradient of the fluid at the cooled surface. Although no clear advantages exist between the different correlations for estimating the N_{Nu} for fluids working beyond the critical point, two non-dimensional quantities are known to be of great relevance for determining the heat transfer mechanism: the Prandtl number N_{Pr} and the Reynolds number N_{Re} which are defined as

$$N_{\mathrm{Pr}} \equiv \frac{\mu C_P}{k} \quad \text{and} \quad N_{\mathrm{Re}} = \frac{GD_\hbar}{\mu}, \text{ respectively,} \tag{8}$$

where μ is the viscosity, C_P is the heat capacity at constant pressure, k the thermal conductivity.

The N_{Pr} and N_{Re} are therefore required to be the same in order to have a similar heat transfer mechanism (at any location) in the reactor and in the downscaled system.

From manipulating the balance equations (1), (3) and (4) a number of dimensionless numbers can be found which determine the constrains in the scaling fluid, the geometrical design and the operational conditions (see Fig. 1). These dimensionless numbers, which have to be kept the same for each relevant section of the loop, are the dimensionless density $\rho^*_{(z)}$ and the dimensionless enthalpy $h^*_{(z)}$, the friction factor f, the Froude number N_{Fr}, the dimensionless hydraulic diameter $D^*_\hbar$, the local friction factors K_i, the dimensionless axial length z^*, the dimensionless cross-sectional area A^*, the dimensionless time t^* and the pseudo phase change number N_{PCH} (only relevant for the core section since the rest of the sections are adiabatic). From the preservation of the heat transfer mechanism, two more dimensionless numbers arise: N_{Pr} and N_{Re}. From all these dimensionless quantities $\rho^*_{(z)}$, $h^*_{(z)}$ and N_{Pr} are used to define the scaling fluid and its operational conditions (see Fig. 1, left-hand side branch).

2.1. Fluid selection and definition of the operational conditions

The fluid will be chosen such that a great reduction in power, pressure and temperature is achieved. In boiling systems it can be assumed that the fluid properties are constant since the fluid is operated roughly at the saturation point, i.e. at the same point in the phase plane. In supercritical systems, however, the fluid properties strongly change when the critical region is crossed. In order to illustrate this effect for water at 25 MPa (the HPLWR nominal pressure) Fig. 2 is constructed.

Water experiences a drastic change in the physical properties such as the density and the enthalpy as the supercritical water is heated from 280 to 500 °C in a HPLWR core. Since the scaling fluid has to behave similarly as water for the whole operational range, the selection of such a fluid and its working conditions is not a straightforward task. An extensive study has been carried out by using the REFPROP v8.0 software package from NIST [10] which allows finding the physical properties of different fluids for a wide range of conditions. Mixture models explicit in Helmholtz energy are implemented in such a program for estimating the physical properties of fluids with mixed components.

As a result, it is found that the combination of refrigerants R-125 and R-32 (22.5/77.5% in mass fraction) at the supercritical pressure of 6.23 MPa can be used to accurately represent supercritical water at the HPLWR working conditions i.e. at P = 25 MPa and between $T_{\mathrm{Core,in}}$ = 280 °C and $T_{\mathrm{Core,out}}$ = 500 °C. A brief comparison between water and the Freon mixture can be found in Table 3 from Appendix. Note that the large database existing for R-32/R-125 mixtures used to create the mixing models implemented in REFPROP, gives a large confidence on the predicting capabilities of this program. For instance, the uncertainties of the calculated mixture density and heat capacity are estimated to be 0.1% and 0.5%, respectively [11].

From the steady state version of Eq. (4) it can be seen that if the same $N_{PCH}(z^*)$ is applied in the reactor and in the downscaled facility, the resulting axial dimensionless enthalpy is also the same. Thus,

$$\frac{\partial}{\partial z^*}(h^*_{(z)}) = N_{PCH}(z) \tag{9}$$

In the case a flat power profile is used in both systems, the dimensionless enthalpy will develop linearly in the core. This result is shown in Fig. 3.

The resulting dimensionless density for water and the proposed mixture plotted in terms of the dimensionless core length are compared in Fig. 4.

In order to show the reduction in temperature obtained by using the proposed mixture of Freons, Fig. 5 is constructed. Clearly,

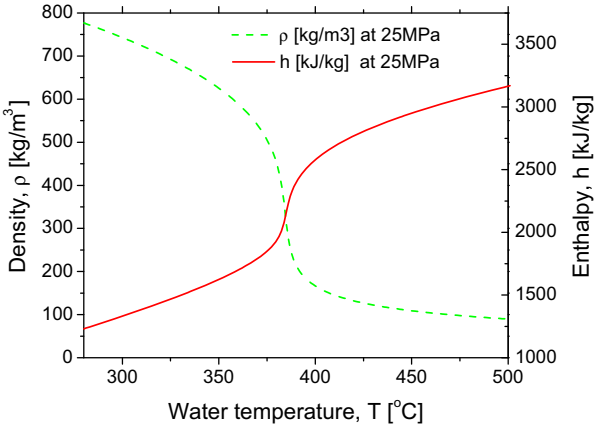

Fig. 2. Variation of ρ and h occurring in the HPLWR core.

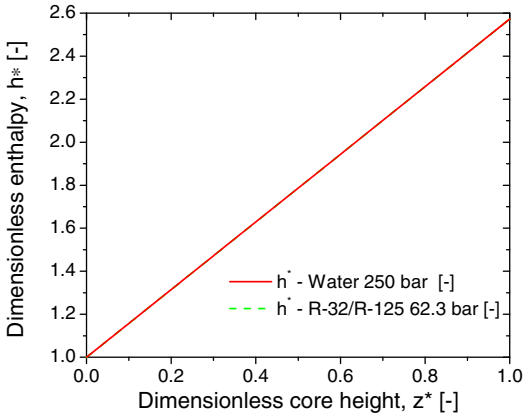

Fig. 3. h_* for water and the proposed Freon mixture at the corresponding working conditions, when a flat power profile is used.

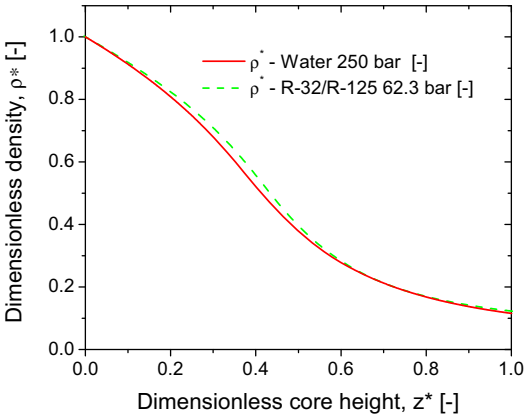

Fig. 4. ρ_* for water and the proposed Freon mixture obtained when a flat power profile is used.

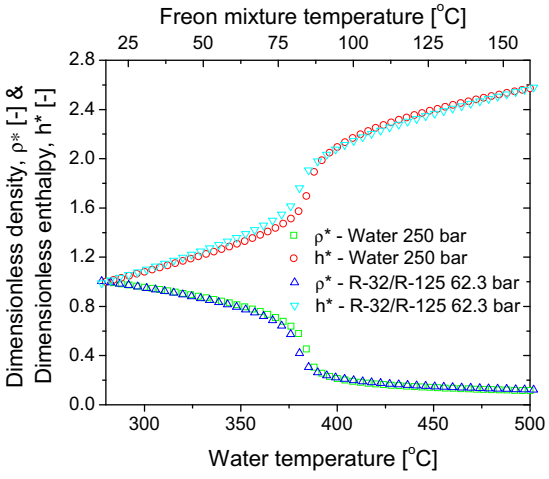

Fig. 5. ρ_* and h_* for water and the proposed Freon mixture in terms of the fluid temperature.

the proposed mixture of Freons provides a very good representation of the dimensionless water density and enthalpy.

Fig. 6 shows the (normalized) C_p plotted in terms of the core axial position. As can be seen the agreement in the location of the transcritical region is excellent.

The Prandtl number for the two fluids is compared in Fig. 7.

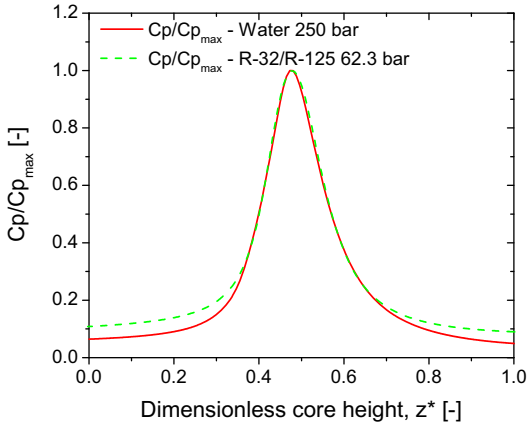

Fig. 6. Normalized C_P for water and the proposed Freon mixture in terms of the fluid temperature.

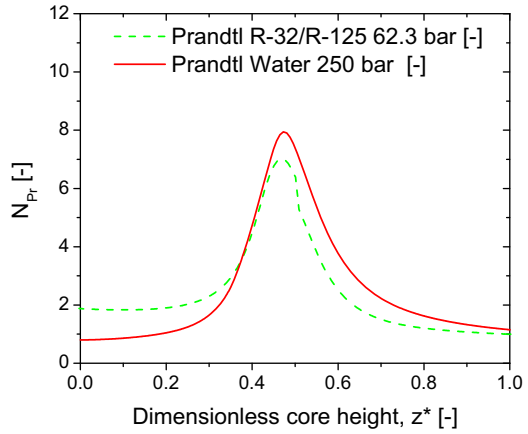

Fig. 7. N_{Pr} along the dimensionless core length z_* for the test facility and the reactor.

2.1.1. Thermal stability of the proposed mixture

In the past, when chlorine-containing refrigerants such as R-11 were in use, the maximum power cycle temperatures had to be limited to 110–120 °C because of the modest molecular stability of the fluids [12]. Nowadays, the phase-out of chlorofluorocarbons has led to large scale availability of HFCs and intense development of fluorinated ethers and other halocarbons. These new, zero ODP chlorine-free hydro-fluorocarbons have the potential of an excellent thermal stability owing to the very strong C–F bond, stronger than both that between C and Cl and between C and H [13]. In particular, several tests done with different hydro-fluorocarbons (HFC) have shown that these type of refrigerants have an excellent thermal stability with a maximum temperature (at which no decomposition signs were detectable) above 300 °C [13].

2.1.2. Comments on the use of CO_2 as scaling fluid of supercritical water

It has to be recalled that some authors have proposed the use of supercritical CO_2 to investigate the stability characteristics of supercritical water systems (see, for instance, Lomperski et al. [14] and Jain [5]). If suitable, CO_2 would be an interesting coolant since it is environmentally friendly, cheap, low risk and its critical point can be reached at low pressures and temperatures. In order to test the suitability of CO_2 for supercritical water stability investigations, Fig. 8 is constructed for this fluid. The CO_2 conditions chosen in Fig. 8 correspond to the operational conditions of the test loop developed by and operated at ANL [5].

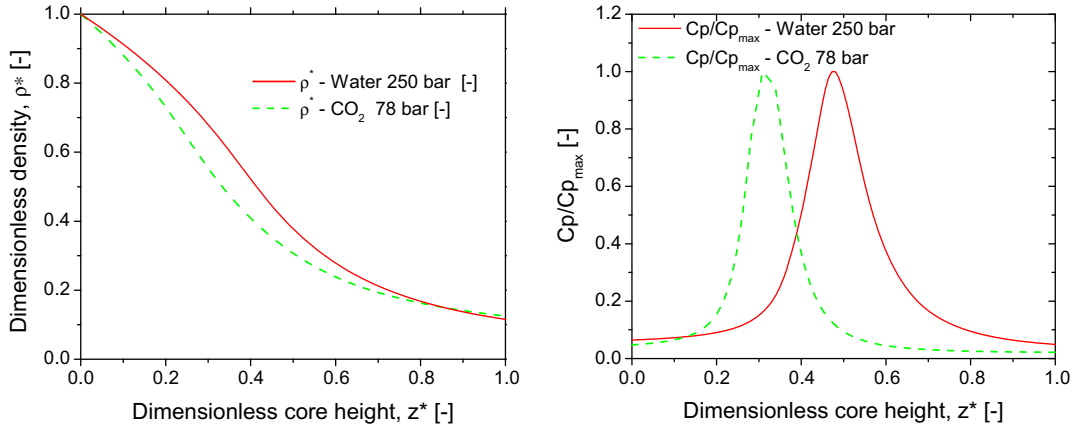

Fig. 8. $\rho*$ and the (normalized) C_p for water and CO_2 at the corresponding working conditions.

Clearly, CO_2 is not a proper model fluid for simulating supercritical water at reactor conditions: the CO_2 $\rho^*(z)$ and $h^*(z)$ do not match those from water. Consequently, a different temperature axial profile is to be expected if the same non-dimensional axial power distribution is applied to the two systems (see Eq. (32) from Appendix). In other words, if the same power profile (in terms of the dimensionless length) would be used for both fluids, the transcritical region will be found at a different location and will have a different shape. This difference may influence the stability of the system. Uncertainties may therefore appear when trying to 'upscale' the CO_2 stability results to water.

2.2. Derivation of the scaling rules from the dimensionless parameters

The loop design derived from the scaling rules is presented in the second and third branch presented in Fig. 1.

2.2.1. Core section

As in the case of BWRs, keeping the same reactor axial frictional pressure drop in the downscaled facility is of importance to keep the same stability performance in both systems. As it will be shown in this section, such a similarity can be achieved with a proper geometrical design of the test facility.

The core geometrical scaling is represented in the second branch of the block diagram of Fig. 1.

In general, the pressure drop caused by fluid flowing at steady state consists of four components: friction, local obstructions, acceleration and gravity. The total pressure drop at supercritical conditions can be estimated by using general correlations developed at subcritical conditions with corrections for the variations in the thermophysical properties and the presence of high heat fluxes [15]. The last effect increases the steep property variations in the channel. The following correlation developed by Filonenko [16] and recommended by Pioro et al. [15] is used for estimating the friction factor

$$f_{(z)} = (1.82\log_{10}(N_{\mathrm{Re}}) - 1.64)^{-2.0} \tag{10}$$

which is recommended for $4\times10^3 < N_{\mathrm{Re}} < 10^{12}$. (11)

It has to be pointed out that the N_{Re} varies along the channel according to axial changes in the dynamic viscosity (the mass flux and the hydraulic diameter remain constant). Therefore, a different axial friction distribution can be found for water and the Freon mixture since the dynamic viscosity was not used in the selection of the scaling fluid.

In order to preserve the axial friction distribution in the core for the two systems as much as possible, core hydraulic diameter in the facility is chosen such that the same dimensionless total friction is created in the core facility and in the reactor core:

$$\int_0^1 f_{(z^*)}dz^*\Big|_{facility,Core} = \int_0^1 f_{(z^*)}dz^*\Big|_{HPLWR,Core} \tag{12}$$

The resulting axial Reynolds number and the friction factor profile for the reactor and the test facility case are shown in Fig. 9.

The Reynolds number for the Freon mixture deviates from the one corresponding to the water case (see left-hand side plot), which is translated into a slightly different axial distribution of the friction factor (see right-hand side plot). From investigations on density wave oscillations occurring in boiling systems, it is known that such a difference can affect the stability similarity between the original system and its downscaled version. In order to compensate for such a difference, the local restrictions K_i (representing the spacers, which also have to be included in the core section) can be used to adjust the profile and to diminish the differences with the reactor.

Once the hydraulic diameter in the test facility core is fixed, the preservation of the Froude number N_{Fr} can be used to determine the core length of the facility.

$$N_{Fr}|_{facility,C} = N_{Fr}|_{HPLWR,C} = \frac{G_0^2}{\rho_0^2 L_c g}\Big|_{HPLWR,C} \tag{13}$$

By using the Reynolds number at core inlet conditions and the dimensionless hydraulic diameter D_h^*, we can rewrite Eq. (13) as

$$N_{Fr}|_{HPLWR,C} = \frac{D_h^*(N_{\mathrm{Re}}\mu)^2\big|_{facility,C,i}}{\rho_0^2 D_h^3 g} \tag{14}$$

which is transformed into

$$D_h|_{facility,C} = \sqrt[3]{\frac{D_h^*(N_{\mathrm{Re}}\mu)^2\big|_{facility,C,i}}{N_{Fr}|_{HPLWR}\rho_0^2 g}} \tag{15}$$

By selecting the reference point to be at the core inlet, the geometrical scaling factor X_g relating the core geometrical dimensions of the reactor and the downscaled system can be found thus as

$$X_g = \frac{L_C|_{facility}}{L_C|_{HPLWR}} = \frac{D_h|_{facility,C}}{D_h|_{HPLWR,C}} = \frac{\sqrt[3]{\frac{(N_{\mathrm{Re}}\mu)^2 D_h^*}{N_{Fr}\rho_0^2 g}\Big|_{facility,C,i}}}{\sqrt[3]{\frac{(N_{\mathrm{Re}}\mu)^2 D_h^*}{N_{Fr}\rho_0^2 g}\Big|_{HPLWR,C,i}}}$$
$$= \sqrt[3]{\frac{(N_{\mathrm{Re}}\mu/\rho)^2|_{facility,C,i}}{(N_{\mathrm{Re}}\mu/\rho)^2|_{HPLWR,C,i}}} = \left(\frac{N_{\mathrm{Re}}v|_{facility,C,i}}{N_{\mathrm{Re}}v|_{HPLWR,C,i}}\right)^{2/3} = 0.78 \tag{16}$$

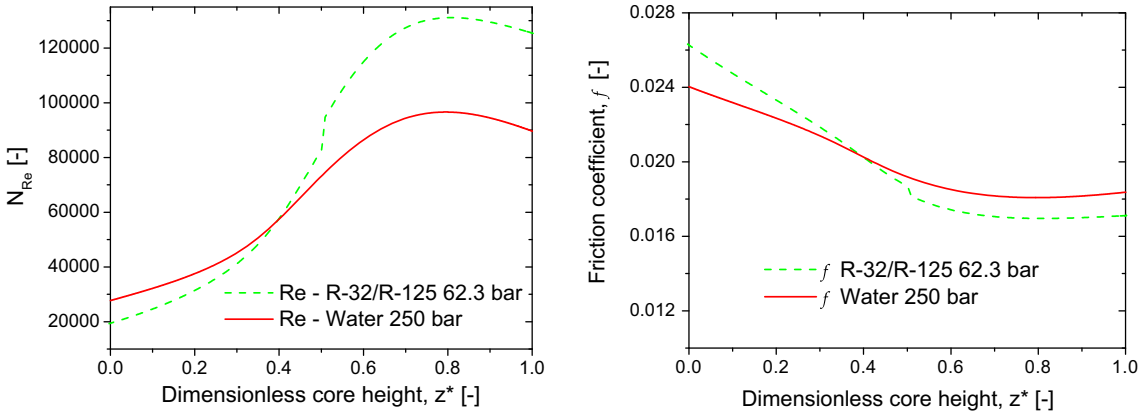

Fig. 9. Variation of N_{Re} and f in terms of the dimensionless core axial position $z*$ for the reactor and the facility.

Note that the second equality holds from the preservation of the dimensionless hydraulic diameter of the core.

When comparing the resulting geometrical scaling rule given by Eq. (16) with the scaling rule for boiling systems, substantial differences can be noted. In the latter case, the preservation of the flow pattern characteristics (described by the Drift-flux model) was chosen to determine the geometrical scaling, while friction effects (which are considered to be less important) could not be scaled [9]. Since there is no flow pattern to preserve in supercritical loops, the friction and the heat transfer mechanism can be properly scaled.

Due to the fact it is not clear which correlation is best for estimating the heat transfer mechanism in the case of supercritical fluids, the well known Dittus–Boelter (developed for boiling systems), expressed in Eq. (17) is used to estimate the Nusselt number N_{Nu}. The comparison of N_{Nu} for the two systems is presented in Fig. 10

$$N_{Nu} = 0.023 N_{Re}^{0.8} N_{Pr}^{0.4} \tag{17}$$

Clearly, a good representation of N_{Nu} is achieved for the downscaling fluid in the whole core.

From Eqs. (13) and (16), the following relation for the mass flux scaling X_G can be found. This derivation is depicted in the second branch of the block diagram of Fig. 1.

$$X_G = \frac{G_0|_{facility,C}}{G_0|_{HPLWR,C}} = \sqrt{\frac{\rho_0^2 L_c|_{facility}}{\rho_0^2 L_c|_{HPLWR}}} = \frac{\rho_0|_{facility}}{\rho_0|_{HPLWR}} X_g^{1/2} = 0.88 \tag{18}$$

From the preservation of the (pseudo) phase change number, the following equation relating the power applied in the original and in the downscaled system can be written

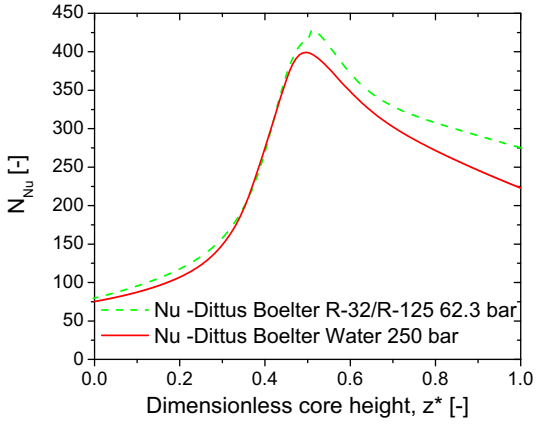

Fig. 10. Evolution of N_{Nu} along the core for water and the proposed mixture of Freons at the corresponding operational conditions.

$$N_{PCH}|_{HPLWR} = N_{PCH}|_{facility} = \left.\frac{q_{tot}}{v_0 \rho_0 h_0 A_c}\right|_{HPLWR} \tag{19}$$

where q_{tot} is the total power applied in the system. Therefore,

$$1 = \frac{\left.\frac{q_{tot}}{G_0 h_0 A_c}\right|_{facility}}{\left.\frac{q_{tot}}{G_0 h_0 A_c}\right|_{HPLWR}} = \frac{q_{tot}|_{facility}}{q_{tot}|_{HPLWR}} \frac{G_0|_{HPLWR}}{G_0|_{facility}} \frac{h_0|_{HPLWR}}{h_0|_{facility}} \frac{A_c|_{HPLWR}}{A_c|_{facility}} \tag{20}$$

The power scaling factor X_{Pow} is given by

$$X_{Pow} = \frac{q_{tot}|_{facility}}{q_{tot}|_{HPLWR}} = \frac{G_0|_{facility}}{G_0|_{HPLWR}} \frac{h_0|_{facility}}{h_0|_{HPLWR}} \frac{A_c|_{facility}}{A_c|_{HPLWR}} = X_G \frac{h_0|_{facility}}{h_0|_{HPLWR}} X_A \tag{21}$$

where the cross-sectional area ratio is

$$X_A = \frac{A_c|_{facility}}{A_c|_{HPLWR}} = X_g^2 = 0.61 \tag{22}$$

Thus,

$$X_{Pow} = 0.089 \tag{23}$$

The (nominal) power per rod that has to be used in the facility can thus be calculated by using Eq. (23).

$$q_{rod}|_{facility} = X_{Pow} q_{rod}|_{HPLWR} = 4.136 \text{ kW} \tag{24}$$

Note that the number of rods that can be used in the test facility depends on the total available power and not on the geometrical design because, in the scaling rules, all the relations are in terms of *normalized* quantities as the hydraulic diameter and the mass flux (see the third branch of the block diagram depicted in Fig. 1). It has to be pointed out that, in practice, only a limited number of heating rods can be simulated in the facility because power limitations. This creates so-called distortions which effect has to be analyzed.

2.2.2. Steam plenum and downcomer

The scaling of the steam plenum (SP) and the downcomer (DC) section is similar to the scaling for the core section (see the third branch of the block diagram of Fig. 1). The only difference is the fact the fluid properties are not varying in these adiabatic sections. The dimensionless density at the core inlet and outlet is the same for water and the mixture of Freons (see Fig. 4) which automatically assures that the densities will also be the same for the SP and the DC sections of the two systems.

The radial scaling of the SP and the DC sections is given by the core cross-sectional area (which depends on the total number of heating rods representing the reactor core). In other words, the ratio between the core sectional area and those from the SP and the DC is kept exactly the same as in the reactor. In this way, the inertia distribution in the reactor is properly simulated by the test facility.

Regarding the friction losses, differences exist in the friction factor at the core inlet (+10%) and outlet (−5%) (see Fig. 9). In the case of the core section, the design of the spacers and the local restrictions can be used to reduce this discrepancy. The aforementioned differences are estimated to cause small deviations for the SP and the DC since the typical hydraulic diameters of these sections are large compared to the one from the core. For this reason, their influence in the total friction is usually not of great relevance in the case of nuclear reactor designs.

Like in the case of boiling loops, it can be shown that by integrating the differential momentum balance equation along the axial direction, the inertia distribution is correctly scaled in the facility if the same geometrical scaling factor is used in the SP, the DC and in the core sections. Moreover, when Eq. (16) is used for the scaling of all dimensions of the loop, the scaling of the time is univocally determined. This characteristic is of importance for keeping the dynamical behavior in the two systems the same [9].

2.2.3. Time scaling from the dimensionless time

From the non-dimensionalizing procedure, the same dimensionless time is found from the three balance equations (mass, momentum and energy) and for all the sections (see the right-hand side branch of the block diagram of Fig. 1). This dimensionless time is expressed as

$$t^* \equiv \frac{t}{\frac{L_C \rho_0}{G_0}} \tag{25}$$

By equalling the dimensionless time for the downscaled system and the reactor, the following relation is obtained for the time ratio X_t,

$$\frac{t|_{facility}}{t|_{HPLWR}} = \frac{G_0}{L_C \rho_0}\bigg|_{HPLWR} \frac{L_C \rho_0}{G_0}\bigg|_{facility} = \frac{G_{0,HPLWR}}{G_{0,facility}} \frac{L_{C,facility}}{L_{C,HPLWR}} \frac{\rho_{0,facility}}{\rho_{0,HPLWR}} \tag{26}$$

And thus,

$$X_t = \frac{t|_{facility}}{t|_{HPLWR}} = X_G^{-1} X_g \frac{\rho_{0,facility}}{\rho_{0,HPLWR}} = 1.2 \tag{27}$$

which shows that the time in the facility runs at a different speed than in the reactor. Note that Eq. (27) has to be used to convert all time-related experimental results to the water time frame.

Table 1 summarizes the scaling procedure by presenting the dimensionless quantities that need to be preserved in each relevant section of the loop.

2.2.4. Margin to the onset of deteriorated heat transfer

At certain high heat flux and low mass flux conditions, a sharp increase in the wall temperature can occur due to the changes in the heat transfer mechanism. This large increase in the wall temperature is referred to '*heat transfer deterioration*' [17]. In the literature there is still no unique definition for the onset of heat transfer deterioration. This is because the reduction in the heat transfer coefficient, or the increase in the wall temperature, behaves rather smoothly compared to the behavior of the boiling crisis at which a much sharper increase in the wall temperature takes place [18]. Up to now, no correlation can accurately predict the onset of deteriorated heat transfer (ODHT). Many authors, however, have found that the ODHT occurs when the ratio given by the heat over the mass flux is larger than a certain value [19]. The following relation is usually used in practice

$$\frac{q''}{G}\Big|_{ODHT} \geq 0.4 \tag{28}$$

where q'' is expressed in kW m^{-2} and G in kg m^{-2} s^{-1}.

In order to estimate the ODHT for the reactor and the test facility, the scaling factors derived previously can be used. Thus,

$$\frac{\frac{q''}{G}\Big|_{ODHT,facility}}{\frac{q''}{G}\Big|_{ODHT,HPLWR}} = X_{Pow} X_q^{-2} X_G^{-1} = 0.16 \tag{29}$$

This result shows that a much larger margin to ODHT is found when the Freon mixture is used instead of water, which enhances the safety of the proposed design.

2.2.5. Scaling of supercritical loops vs. scaling of boiling loops

In this section, a brief comparison is assessed between the fluid-to-fluid scaling of natural circulation supercritical loops and the scaling of natural circulation boiling loops. Details regarding the last approach can be found in Marcel et al. [9]. To clarify the differences between the two downscaling methods, Table 2 summarizes the phenomena which are preserved and the resulting scaling factors obtained for typical values corresponding to reactor nominal conditions. The proposed mixture of Freons is used to scale the HPLWR and Freon R-134a is used in the case of the boiling water reactor.

The main differences and analogies between the two scaling approaches are listed below.

In boiling loops almost any fluid can be used as scaling fluid (as far as the desired density ratio is matched).

In the supercritical case, however, the constraints on the fluid are more difficult to satisfy (namely the shape of the dimensionless density and enthalpy along the loop) and therefore, a limited number (or combination) of fluids can be used from which only few may be useful in practice.

Another difference refers to the geometrical scaling. In boiling loops the focus is on the proper simulation of the flow pattern and its transitions, in which the key fluid parameter is the surface tension. A correct simulation of the flow pattern determines the geometrical scaling which is not present in the case of supercritical loops.

Since there is no flow pattern to preserve in a supercritical fluid, more attention can be given to the proper simulation of the friction distribution in the loop and the heat transfer mechanism.

In both systems a unique geometrical scaling factor has to be used for all sections which assures the inertia distribution in the reactor will be preserved in the loop.

3. Conclusions

The aim of this work was to develop scaling rules allowing downscaling of a water loop with supercritical water by using fluid-to-fluid modeling. Those rules were used to design a test facility suitable for investigations on the dynamics of the supercritical light water reactor. The High Performance Light Water Reactor is therefore taken as the reference reactor in this paper. Aim is to select a proper fluid that allows simulating the HPLWR by using much less severe conditions.

Scaling rules were derived from the dimensionless mass, momentum and energy balance equations and their boundary

Table 1
Dimensionless quantities to be preserved in each relevant section of the system.

	Core	Steam plenum[a]	Downcomer
Quantities to be preserved	$\rho*$, $h*$, f, N_{Fr}, D_h*, $A*$, K_i, $z*$, N_{PCH}, N_{Nu}	f, N_{Fr}, D_h*, $A*$, K_i, $z*$	f, N_{Fr}, K_i, D_h*, $A*$, $z*$

[a] Although there is no *steam* in the HPLWR, the section above the core is referred in literature as steam plenum.

Table 2
Differences between the fluid-to-fluid scaling method for simulating supercritical loops and boiling loops.

Item	NC – supercritical loops (R-32/R-125)		NC – boiling loops (R-134a)	
Fluid selection	Given by the evolution of $\rho_{*(z^*)}$, $h_{*(z^*)}$	$X_{Press} \approx 0.25$	Given by the density number; N_ρ	$X_P \approx 0.017$
Flow pattern	–	–	Scaled by the drift-flux parameters and thus N_{We} and N_{Fr}	–
Core radial geometry	Given by the friction in the core; $f(N_{Re})$	$X_g \approx 0.78$	Given by the flow pattern preservation; N_{We}, N_{Fr}, N_{Pe}	$X_g \approx 0.46$
Axial geometry	Scaled the buoyancy forces; N_{Fr}		Scales the buoyancy forces; N_{Fr}	
Radial scaling	Gives the proper inertia distribution		Gives the proper inertia distribution	
Friction	Scaled; $f(N_{Re})$		Distortion	
Power	Scaled; (pseudo) N_{PCH}	$X_{Pow} \approx 0.09$	Scaled; N_{PCH}	$X_{Pow} \approx 0.02$
Heat transfer	Scaled; N_{Nu}		Distortion	
Time scaling	Scaled; $t*$	$X_t \approx 1.2$	Scaled; $t*$	$X_t \approx 0.68$

X_P being the pressure scaling factor and N_ρ the density number, N_{We} the Weber number and N_{Pe} the Peclet number.

conditions, which needed to be similar for both the HPLWR and the downscaled facility. From those rules it is found that the dimensionless density and enthalpy variations, together with the Prandtl and Reynolds numbers, need to be the same at any point (in terms of the dimensionless axial position) in both the original and in the downscaled system. Such conditions imply hard constrains on the scaling fluid used for representing supercritical water.

In the case of supercritical water at the HPLWR conditions, it is found that a mixture of Freons R-32 and R-125 (77.5/22.5% mass fraction) at 6.23 MPa can accurately simulate the dimensionless density and enthalpy variations in the reactor core. The proposed coolant allows a considerable reduction in power, operational pressure and temperature.

From the balance equations it is found that the radial scaling of the test facility can be used to adjust the friction distribution in the loop. As a result, a good representation of the frictional pressure drops can be obtained. By fixing the radial dimensions, the lengths are determined by using a unique geometrical scaling rule. By doing so, exactly the same inertia distribution is obtained in the HPLWR and its downscaled version.

As in the case of fluid-to-fluid scaling of boiling loops, the time is not scaled one-to-one in the original system and its downscaled version but the time in the last case runs faster.

From the boundary condition it arose that to preserve the heat transfer mechanism, two non-dimensional quantities have to be preserved: the Reynolds number (already used to model the friction distribution in the loop) and the Prandtl number (also used in the selection of the downscaling fluid). It is found that the mixture of fluids with the scaling proposed in this work can simulate the Nusselt number reasonably well, which assures a good simulation of the heat transfer mechanism.

As a side step, it was found that supercritical CO_2 cannot accurately simulate supercritical water at HPLWR conditions. Consequently, care has to be taken when using CO_2 experiments to draw conclusions regarding the stability of supercritical water based reactors.

Table 3
Reactor and test facility main data and physical properties of water and the proposed Freon mixture at the corresponding operational conditions.

	Water – HPLWR	Freon mixture – test facility
Composition (mass fractions)	100% H_2O	77.5% R-32; 22.5% R-125
Critical pressure (MPa)	22.06	5.38
Operational pressure (MPa)	25.0	6.23
Inlet temperature[a] (°C)	280	17.5
Outlet temperature[a] (°C)	500	158.9
Density[a] (kg m^{-3})	777.0	1061.9
Enthalpy[a] (kJ kg^{-1})	1230.5	229.04
Viscosity[a] (μPa s)	99.114	133.71
Chemical stability	Stable	Flammable at $T > 648$ °C

[a] Regarding the core inlet; estimated by using REFPROP v8.0.

Appendix A

The physical properties of the coolants used in the HPLWR and in the proposed test facility are given in Table 3.

Dimensionless version of the heat transfer equations.

In a channel, the radial temperature gradient is related to the heat flux on the surface of the heating rod by the liquid thermal conductivity as

$$q''_{(z^*)} = k_{(z^*)} \left.\frac{\partial T_{(z^*)}}{\partial r}\right|_{r=r_0} \tag{30}$$

The convection heat transfer is given by

$$q''_{(z^*)} = h_{(z^*)}(T_{s(z^*)} - T_{m(z^*)}) \tag{31}$$

From Eqs. (30) and (31), the following can be written

$$k_{(z^*)} \left.\frac{\partial T_{(z^*)}}{\partial r}\right|_{r=r_0} = h_{(z^*)}(T_{s(z^*)} - T_{m(z^*)}) \tag{32}$$

Rearranging Eq. (32) we find

$$\left.\frac{\partial T_{(z^*)}}{\partial r/r_0}\right|_{r=r_0} \frac{1}{(T_{s(z^*)} - T_{m(z^*)})} = \frac{h_{(z^*)}}{k_{(z^*)}} r_0 \tag{33}$$

which in its non-dimensional version is written as

$$\left.\frac{\partial T^*_{(z^*)}}{\partial r^*}\right|_{r=r_0} \frac{1}{(T^*_{s(z^*)} - T^*_{m(z^*)})} = \frac{Nu_{(z^*)}}{2} \tag{34}$$

References

[1] Generation IV International Forum (GIF), A technology roadmap for the Generation IV nuclear energy systems, GIF-002-00, 2002.
[2] G. Yadigaroglu, Two-phase Flow Instabilities and Propagation Phenomena, Hemisphere Publishing Corporation, 1981 (Chapter 17, pp. 353–403).
[3] J. Hofmeister, T. Schulenberg, J. Starflinger, Optimization of a Fuel Assembly for a HPLWR, Proceedings of ICAPP2005, Paper No. 5077, Seoul, Korea, 2005.
[4] V. Chatoorgoon, A. Voodi, P. Upadhye, The stability boundary for supercritical flow in natural convection loops part II: CO_2 and H_2, Nucl. Eng. Des. 235 (24) (2005) 2581–2593.
[5] R. Jain, Thermal-hydraulic instabilities in natural circulation flow loops under supercritical conditions, PhD Thesis, University of Wisconsin, Madison, USA, 2005.
[6] T. Ortega Gómez, A. Class, R.T. Lahey Jr., T. Schulenberg, Stability Analysis of a Uniformly Heated Channel with Supercritical Water, Proceedings of ICONE 14, July 17–20, Miami, FL, USA, Paper 89733, 2006.
[7] R.T. Lahey, F.J. Moody, The Thermal-hydraulics of a Boiling Water Reactor, American Nuclear Society Publisher, 1993.
[8] R. Van de Graaf, T.H.J.J. Van der Hagen, Two-phase flow scaling laws for a simulated BWR assembly, Nucl. Eng. Des. 148 (1994) 455–462.
[9] C.P. Marcel, M. Rohde, T.H.J.J. Van der Hagen, Fluid-to-fluid modeling of natural circulation boiling loops for stability analysis, Int. J. Heat Mass Transfer 51 (2008) 566–575.
[10] E.W. Lemmon, M.O. McLinden, M.L. Huber, NIST Reference Fluid Thermodynamic and Transport Properties – REFPROP, version 8.0. US Department of Commerce, Technology Administration, National Institute of Standards and Technology, 2007.
[11] E. Lemmon, R. Jacobsen, Equations of state for mixtures of R-32, R-125, R-134a, R-143a, and R-152a, J. Phys. Chem. Ref. Data 33 (2) (2004) 593–620.

[12] L. Calderazzi, P. Colonna di Paliano, Thermal stability of R-134a, R-141b, R-1311, R-7146, R-125 associated with stainless steel as a containing material, Int. J. Refrig. 20 (6) (1997) 381–389.
[13] G. Angelino, C. Invernizzi, Experimental investigation on the thermal stability of some new zero ODP refrigerants, Int. J. Refrig. 26 (2003) 51–58.
[14] S. Lomperski, D. Cho, R. Jain, M. Corradini, Stability of a Natural Circulation Loop with a Fluid Heated Through the Thermodynamic Pseudocritical Point, Proceedings of ICAPP Pittsburgh, PA, USA, June 13–17, 2004, Paper 4268, 2004.
[15] I.L. Pioro, R. Duffey, T. Dumouchel, Hydraulic resistance of fluids flowing in channels at supercritical pressures (survey), Nucl. Eng. Des. 231 (2004) 187–197.
[16] G.K. Filonenko, Hydraulic resistance of the pipelines, Therm. Eng. 4 (1954) 40–44 (in Russian).
[17] B.S. Shiralkar, P. Griffith, Deterioration in heat transfer to fluids at supercritical pressure and high heat fluxes, J. Heat Transfer (1969) 27–36.
[18] X. Cheng, T. Schulenberg, A. Souyri, V. Sanchez, N. Aksan, Heat Transfer and Pressure Drop at Supercritical Pressure – Literature Review and Application to an HPLWR (Deliverable D7) – Contract No. FIKI-CT-2000-00033, 2001.
[19] I. Pioro, H. Khartabil, R. Duffey, Heat transfer to supercritical fluids flowing in channels – empirical correlations (survey), Nucl. Eng. Des. 230 (2004) 69–91.